Supplemental Material
for

A study on harmonizing total column ozone assimilation with multiple sensors

Yves J. Rochon[1], Michael Sitwell[1] and Young-Min Cho[2]

[1]Atmospheric Science and Technology Directorate, Environment and Climate Change Canada, Toronto, M3H 5T4, Canada
[2]Centre for Research in Earth and Space Science, York University, Toronto, M3J 1P3, Canada

Correspondence to: Yves J. Rochon (yves.rochon@canada.ca)

Submitted to the Atmos. Chem. Phys. Journal, 2018

The supplemental material contains three complementary tables on comparisons of OMI and ground-based total column ozone measurements, followed by 20 complementary figures covering different topics, and the data graphically represented in the figures of the paper.

Region	Station name	WMO ID⁺	Latitude (deg)	Longitude (deg)	Elevation (m)	Mean differences (%) [# of points] Summer 2014	Summer 2015	Winter 2015
North America and Greenland	Alert	018	82.45	-62.51	220	0.65 [47]	-0.49 [43]	
	Edmonton	021	53.55	-114.11	752	2.34 [53]	2.60 [103]	1.12 [73]
	Resolute	024	74.71	-94.97	68	0.56 [36]	0.35 [102]	
	Toronto	065	43.78	-79.47	202	0.99 [53]		
	Goose Bay	076	53.31	-60.36	26	0.72 [62]	1.94 [92]	0.21 [63]
	Churchil	077	58.74	-94.07	26	0.81 [50]	-0.31 [95]	0.85 [55]
	Saturna Island	290	48.78	-123.13	202	1.74 [53]	1.05 [102]	0.94 [50]
	Eureka	315	79.99	-85.93	8	-0.61 [53]	-1.36 [104]	
	Bondville	357	40.05	-88.37	213	-0.26 [8]	0.67 [46]	-0.52 [25]
	Boulder	424	40.13	-105.24	1689	0.18 [150]	1.41 [137]	-0.20 [96]
	Raleigh	461	35.73	-78.68	272	*4.30 [4]	-3.14 [46]	0.79 [32]
	Fort Peck	362	48.31	-105.10	634		-3.50 [46]	1.97 [37]
	Houston	484	29.72	-95.34	64		0.12 [49]	-1.23 [27]
	Rocky Mountain	392	40.03	-105.53	2923	2.14 [53]	*4.03 [44]	-1.93 [35]
	Sondrestrom	267	67.00	-50.62	300	-1.42 [51]	-1.38 [55]	-2.38 [2]
Europe and Africa	Uccle	053	50.80	4.35	100	-0.87 [134]		
	Hradec Kralove	096	50.18	15.84	285	-1.42 [149]	-0.82 [119]	0.06 [83]
	Hohenpeissenberg	099	47.81	11.01	975	0.59 [47]	0.53 [50]	0.91 [40]
	Oslo	165	59.94	10.72	90	-0.93 [54]	-1.28 [48]	-1.72 [10]
	Norrkoeping	279	58.58	16.15	43	-2.40 [56]	-2.35 [28]	-0.40 [15]
	Vindeln	284	64.24	19.77	225	-0.22 [49]	1.08 [24]	-0.13 [7]
	Valentia Observatory	318	51.93	-10.25	14	1.72 [103]	1.88 [49]	0.94 [35]
	Poprad-Ganovce	331	49.03	20.32	706	-0.99 [42]	-0.42 [52]	-0.44 [29]
	Thessaloniki	261	40.52	22.97	50	-0.49 [45]	-0.58 [48]	-1.85 [24]
	Kislovodsk	282	43.73	42.66	2070	2.80 [48]	2.42 [42]	-1.03 [7]
	Rome	305	41.90	12.50	75	-0.23 [55]	0.33 [44]	0.77 [38]
	Obninsk	307	55.10	36.61	100	-1.07 [57]	-1.09 [52]	-0.76 [14]
	De Bilt	316	52.10	5.18	24	-2.29 [54]	-1.39 [48]	-2.49 [31]
	Reading	353	51.44	-0.94	66	2.14 [112]	0.43 [46]	0.85 [33]
	Andoya	476	69.28	16.01	380	-1.03 [22]	-1.50 [33]	
	Murcia	346	38.00	-1.16	69	-0.07 [54]		
	Manchester	352	53.47	-2.23	76	-0.65 [47]	-0.47 [51]	-1.78 [19]
	La Coruña	405	43.33	-8.41	65	*-5.00 [25]		
	Zaragoza	411	41.63	-0.88	258	-0.37 [53]		
	Aosta	479	45.74	7.36	570	-0.73 [101]	-0.99 [46]	-1.24 [42]
	Tamanrasset	002	22.78	5.52	1384	-1.84 [54]		-0.71 [45]
	Marsa Matrüh	376	31.33	27.22	35	-2.41 [53]		
East Asia	Petaling Jaya	322	3.10	101.65	86	1.58 [82]		1.18 [45]
	Pohang	332	36.03	129.38	6	-0.90 [25]		
	Minamitorishin	030	24.29	153.98	9	-0.73 [55]	-1.29 [47]	-0.40 [40]
	Mt. Waliguan	295	36.29	100.90	3810		*7.36 [42]	*-4.06 [21]
	Linan	325	30.18	119.44	132		-1.87 [32]	*-5.38 [26]
	Longfengshan	326	44.73	127.59	334		*4.15 [48]	*-21.47 [40]
	Lhasa	349	29.67	91.13	3650		*10.59 [48]	1.48 [41]
	Songkhla	345	7.20	100.60	12		-0.99 [30]	-1.24 [37]
	Bangna Bangkok	216	13.67	100.62	60			-2.20 [43]
	Anmyeon-do	513	36.54	126.33	57	-0.87 [45]		
Other	Mauna Loa	031	19.54	-155.58	3397	3.10 [53]	*4.99 [47]	*5.08 [84]
	Paramaribo	435	5.81	-55.22	16	-0.45 [52]	0.08 [39]	0.88 [36]
	Zhongshan	478	-69.37	-76.38	11			*-5.68 [51]
	Amundsen-Scott	111	-90.00	70.24	3507			-2.17 [55]
	Marambio	233	-64.23	-56.62	198	*-5.90 [13]		0.67 [46]

⁺World Meterological Organization station identification number

*Identifies stations with outlier mean differences as either larger in size than 6 % or exceeding two standard deviations of the mean difference variability standard deviation over all remaining stations.

Table S1. List of time mean differences of total column ozone between OMI-TOMS and Brewer stations over July-August 2014/2015 and January-February 2015. The Bandung station, Indonesia, is not included as it was later found to have been assigned incorrect coordinates.

Region	Station name	WMO ID+	Latitude (deg)	Longitude (deg)	Elevation (m)	Mean differences (%) [# of points]		
						Summer 2014	Summer 2015	Winter 2015
North America and Greenland	Caribou	020	46.87	68.03	192		1.32 [11]	
	Boulder	067	40.01	-105.25	1689	-0.43 [65]	-1.06 [52]	-0.22 [39]
	Wallops	107	37.93	-75.48	13	0.26 [18]		
	Mexico City	192	19.33	-99.18	2268		*-7.57 [10]	*-4.67 [14]
	Barrow	199	71.32	-156.61	11	-1.09 [25]	-1.16 [16]	
	La Habana	311	23.14	-82.34	50	-1.43 [27]	-0.86 [5]	0.26 [12]
	Hanford	341	36.32	-119.63	73	-0.25 [32]		0.72 [22]
Europe and Africa	Tamanrasset	002	22.78	5.52	1382	-2.12 [53]	-1.82 [49]	-0.19 [46]
	Haute Provence	040	43.93	5.70	684	-0.36 [49]	1.85 [47]	
	Lerwick	043	60.13	-1.18	82	0.02 [12]		
	Hradec Kralove	096	50.18	15.84	285	-0.74 [24]	-0.77 [25]	1.71 [6]
	Hohenpeissenberg	099	47.81	11.01	975	0.13 [20]	0.13 [30]	1.18 [18]
	Fairbanks	105	64.82	-147.87	138	-2.78 [27]		
	Nashville	106	36.25	-86.57	182	0.15 [79]	-1.79 [23]	0.71 [23]
	Biscarrosse	197	46.77	-100.76	511		0.56 [12]	-0.55 [13]
	Bucharest	226	44.48	26.13	100	-0.86 [11]	-0.22 [9]	0.99 [11]
	Aswan	245	23.97	32.78	190	-1.32 [10]		
	Vindeln	284	64.24	19.77	225		-1.19 [13]	
	Athens	293	37.98	23.73	280	1.55 [38]	1.64 [34]	
	Hurghada	409	27.28	33.75	7	-1.91 [50]		
	Amberd	410	40.38	44.25	2070	*6.70 [41]		
	Kyiv-Goloseyev	498	50.36	30.50	206	0.18 [27]	1.46 [51]	2.83 [18]
East Asia	Sapporo	012	43.06	141.33	26	-0.52 [25]	0.80 [13]	1.51 [11]
	Tateno	014	36.06	140.13	31	1.24 [22]	1.78 [16]	0.03 [26]
	Naha	190	26.21	127.69	28	1.18 [22]	2.72 [11]	1.12 [11]
	Xhianghe	208	39.75	116.96	29	0.01 [11]	-0.09 [5]	
	Kunming	209	25.03	102.68	1891	*-4.21 [10]		
	Bangna Bangkok	216	13.67	100.61	53	-2.43 [2]	-2.92 [2]	-2.48 [1]
Other	Mauna Loa	031	19.53	-155.58	3400	3.52 [92]	1.35 [24]	3.40 [56]
	Buenos Aires	091	-34.58	-58.48	25	-0.37 [46]		
	Syowa	101	-69.01	39.58	22	-3.37 [2]	*-4.27 [2]	-0.13 [22]
	Amundsen-Scott	111	-89.98	-24.80	2810			-1.52 [75]
	Perith	159	-31.92	115.96	2	0.87 [36]	-0.84 [13]	0.18 [64]
	Cachoeira	200	-22.69	-45.01	574	-2.27 [14]	-2.08 [31]	*-5.44 [28]
	Natal	219	-5.84	-35.21	49		-0.64 [26]	-1.71 [23]
	Marambio	233	-64.23	-56.62	198	-3.30 [4]		1.74 [37]
	Lauder	256	-45.04	169.68	370	0.06 [18]	-0.27 [15]	0.56 [18]
	Ushuaia	339	-54.85	-68.31	17	-1.64 [35]	-0.96 [41]	-0.83 [46]
	Comodoro	342	-45.78	-67.50	46	-0.61 [32]	-1.32 [42]	1.46 [43]
	La Quiaca	513	-22.11	-65.44	3459		-0.70 [52]	

+ World Meterological Organization station identification number

*Identifies stations with outlier mean differences as either larger in size than 6 % or exceeding two standard deviations of the mean difference variability standard deviation over all remaining stations.

Table S2. List of time mean differences of total column ozone between OMI-TOMS and Dobson stations over July-August 2014/2015 and January-February 2015. The Dobson total column ozone measurements for the two summer periods were adjusted according to the bias correction equation as a function of the ozone effective temperature. Those for the winter period were not adjusted in the absence of the ozone effective temperature for the period. The impacts of the corrections on the mean differences for the Dobson summer periods were reductions between 0.0 and 0.4 %. The Samoa station, which is part of the WOUDC network, is not included as we had associated incorrect coordinates to it.

Region	Station name	WMO ID+	Latitude (deg)	Longitude (deg)	Elevation (m)	Mean differences (%) [# of points]		
						Summer 2014	Summer 2015	Winter 2015
Russia	Almaty	003	43.14	76.56	847	-0.46 [5]	-3.04 [13]	
	Vladivostok	016	43.12	131.90	138		-1.33 [4]	-2.06 [2]
	St. Pertersburg	042	59.95	30.70	74	-2.09 [6]	*-3.60 [5]	
	Bolshaya Elan	112	46.95	142.70	22		-1.60 [1]	
	Samara	115	53.25	50.22	139	1.34 [13]	2.61 [9]	
	Moscow	116	55.75	37.57	187	0.56 [4]		
	Murmansk	117	68.97	33.05	46	-1.75 [10]	-0.42 [9]	
	Nagaevo	118	59.55	150.78	115	1.00 [2]	0.78 [2]	
	Omsk	120	55.02	73.38	100	-2.24 [8]	-1.71 [7]	
	Yekaterinburg	122	56.73	61.07	300	-2.91 [2]	0.55 [7]	
	Yakutsk	123	62.02	129.72	100	-1.26 [3]	-1.33 [3]	
	Pechora	129	65.12	57.10	61	-2.47 [8]		
	Petropavko	130	53.08	158.55	78	0.62 [10]	0.83 [10]	-0.14 [5]
	Turuhansk	142	65.47	87.56	0		-2.41 [4]	
	Krasnoyars	143	56.00	92.88	277	-2.09 [1]	-1.60 [4]	
	Vitim	148	59.45	112.58	200	-1.28 [3]	-1.36 [4]	
	Hanty-Mansijsk	150	60.97	69.00	40	-0.42 [3]		
	Atiray	183	47.07	51.53	24		-0.57 [1]	
	Tiksi	186	71.58	128.90	0	2.03 [1]		
	Arkhangel’sk	271	64.55	40.58	0	-1.07 [22]	*-4.32 [4]	

+ World Meterological Organization station identification number

Table S3. List of time mean differences of total column ozone between OMI-TOMS, and filter ozonometer stations over July-August 2014/2015 and January-February 2015.

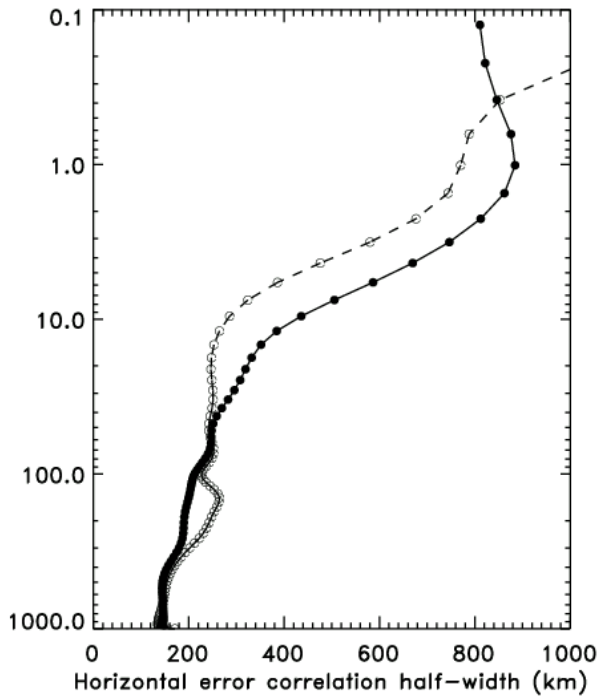

Figure S1. Half-width at half-maximum (HWHM) values (km) for the third order autoregressive (TOAR) correlation model representing the horizontal ozone forecast error correlations derived from 48-24hr forecast differences (dashed) and 6hr time differences of the free running LINOZ ozone model (solid). The vertical axis is equivalent to pressure in hPa for a surface pressure of 1013.5 hPa.

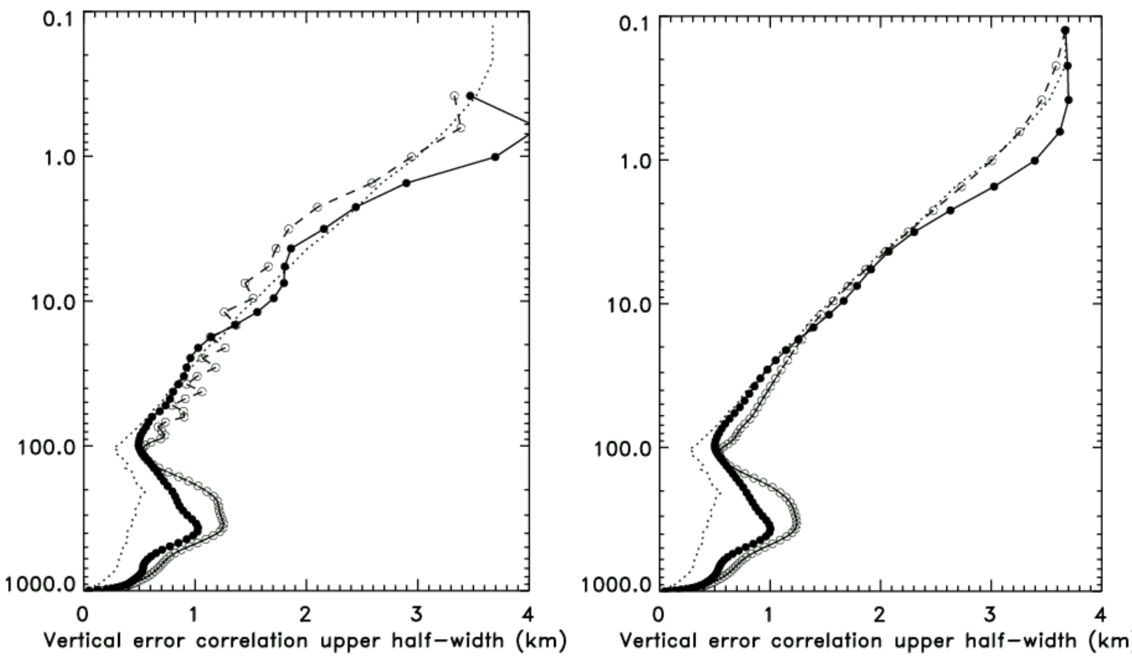

Figure S2. Upper half-width at half-maximum (HWHM) values (km) for the third order autoregressive correlation model representing the vertical ozone forecast error correlations derived from 24-48hr forecast differences (dashed) and 6hr time differences of the free running LINOZ ozone model (solid). The dashed curve presents the approximate local vertical model resolution for the version of the model for which the correlations were derived. The vertical axis is equivalent to pressure in hPa for a surface pressure of 1013.5 hPa. The curves on the left panel show the initially obtained values and those on the right panel are the final values after imposing lower limits equal to separation between adjacent levels and localized vertical filtering. The vertical correlation HWHM were derived in natural logarithm of pressure and, for plotting purposes only, approximately converted to kilometers using the ideal gas law and an isothermal temperature of 220 Kelvin.

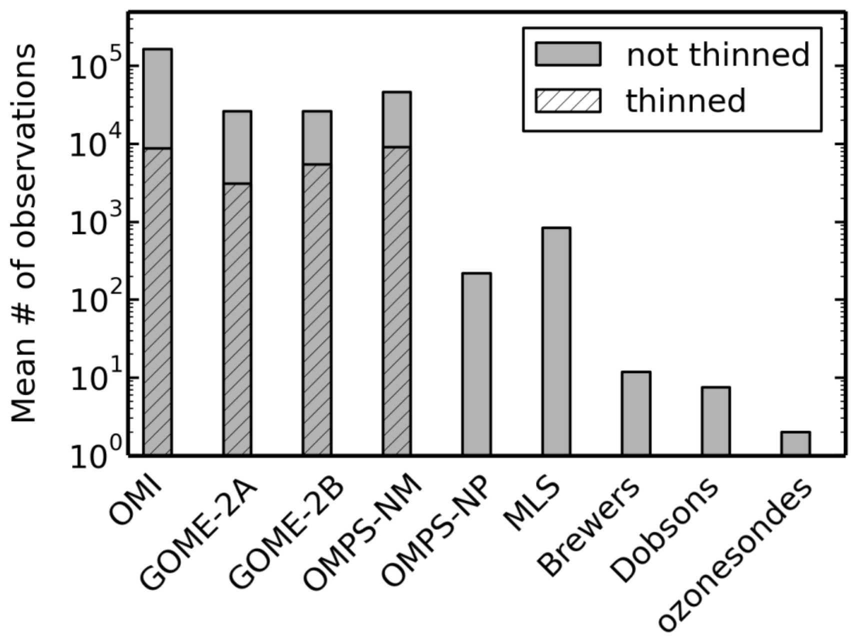

Figure S3. Mean number of observations in 6 hour intervals during the time period July-August 2014 for satellite and ground-based total ozone column instruments, sample profiler satellite instruments, and ozonesondes. Thinning is done to a 1° separation between measurements for total column ozone instruments.

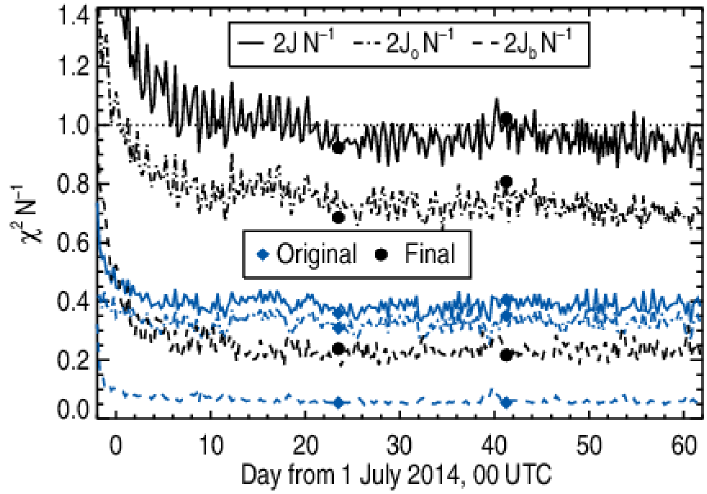

Figure S4. Time series of normalized total chi-squares $2JN^{-1}$ (unitless) and its components for differences from observations $2J_oN^{-1}$ and forecasts $2J_bN^{-1}$ covering all of July and August 2014 with a starting date of 29 June 2014. The number N denotes the total number of assimlated total column ozone data. The two sets of curves stem from use of the original and updated (final) forecast and total column observation error standard deviations.

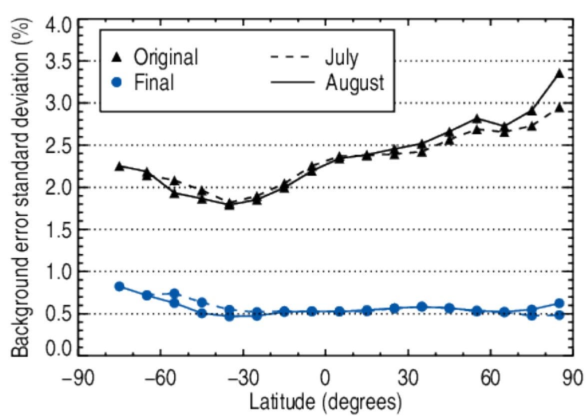

Figure S5. Original and updated (final) set of total column background error standard deviations (%) obtained from projecting the applied latitude and vertically dependent background ozone error variances and the globally homogeneous background vertical error correlations to the total ozone observation space as a function of latitude (degrees) for July and August.

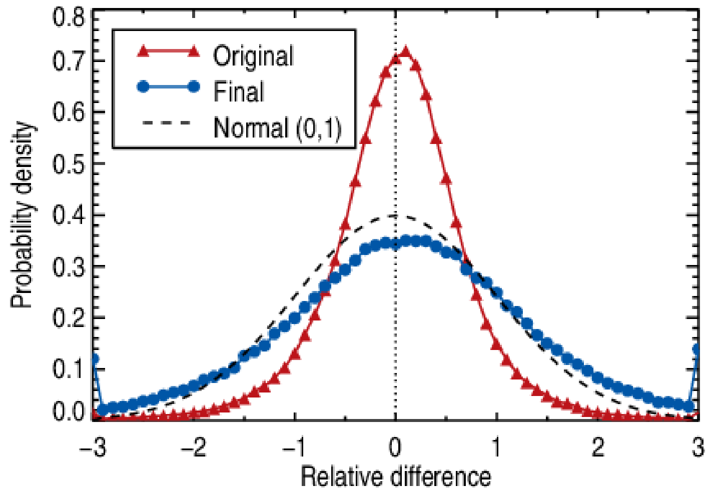

Figure S6. Probability density functions of observation minus forecast relative differences $(O\text{-}F)(\sigma_o^2 + \sigma_b^2)^{-0.5}$ (unitless) following the application of the original and updated (final) observation and background error standard deviations as compared to the normal gaussian distribution. The values at the end points are accumulated values over the wings of the distribution. The differences were taken over all four sets of total column obsevations for a sample four day period covering 4 to 7 August 2014.

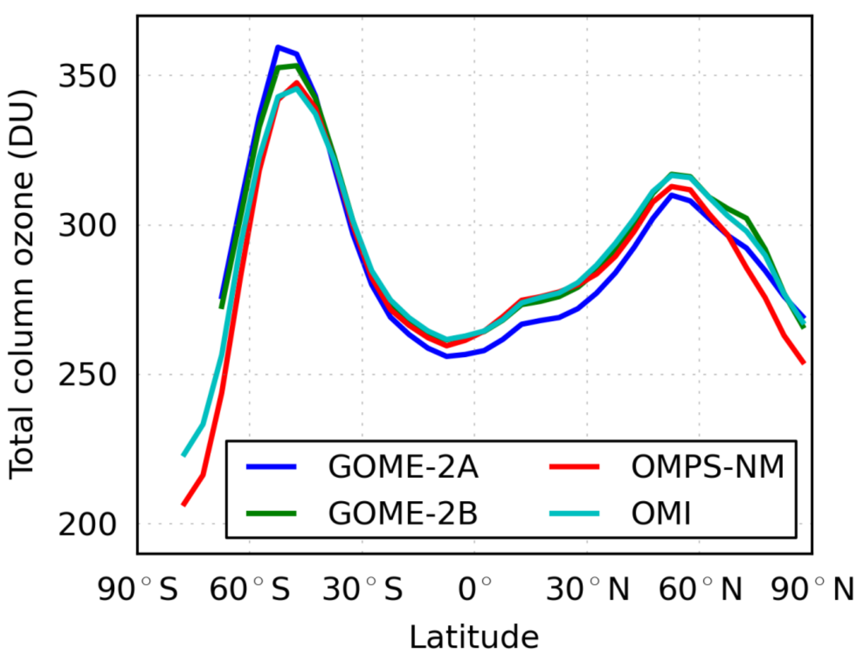

Figure S7. Total column ozone zonal means (DU) as a function of latitude (degrees), using 5° bins, for August 2014. This shows average latitudinal differences between instrumetnts and allows an approximate conversion between percentage and absolute differences for Fig. 3, for example.

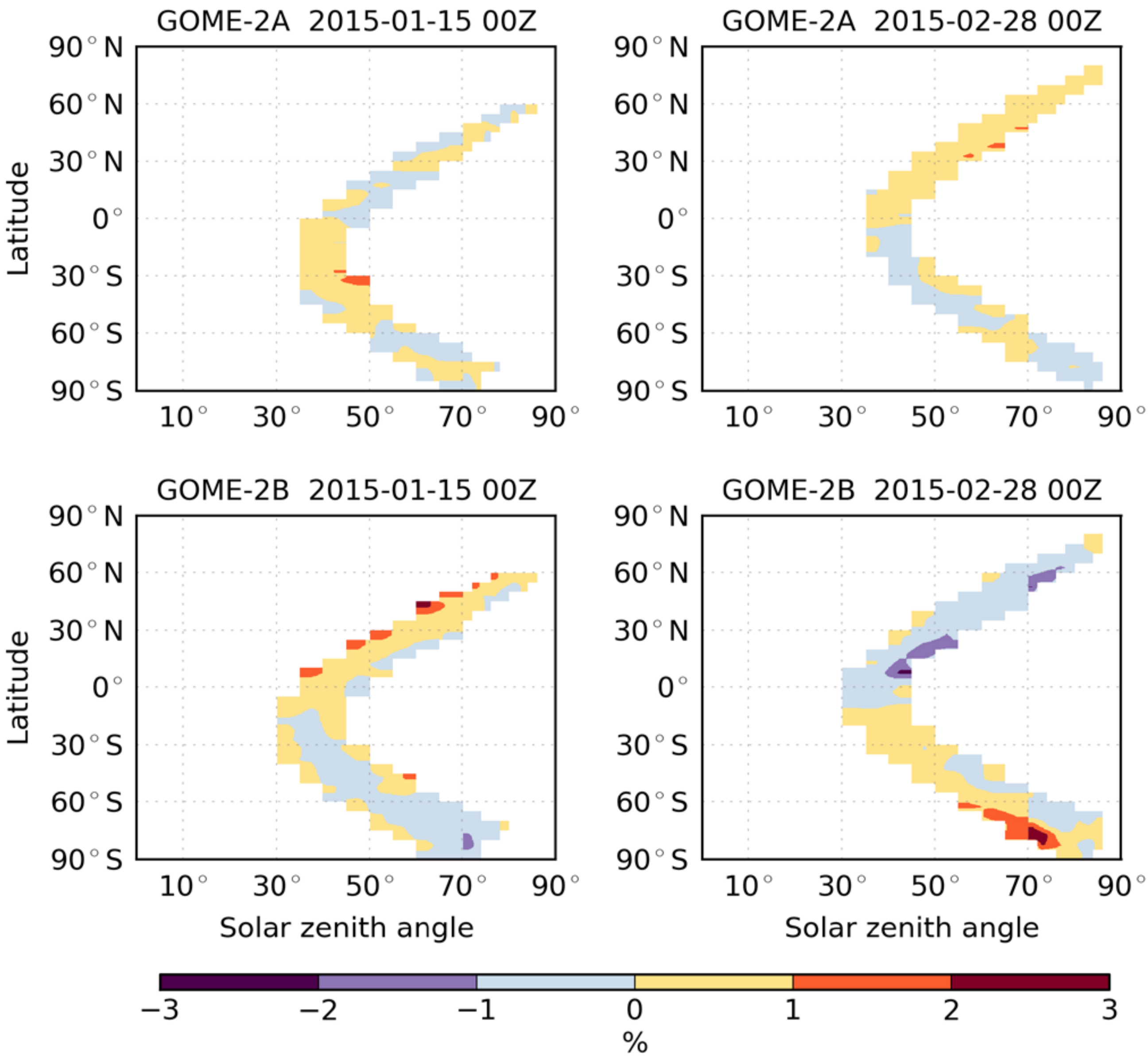

Figure S8. Differences (%) between the time mean bias corrections and the individual time dependent bias corrections for GOME-2A (top row) and GOME-2B (bottom row). The time mean bias corrections are over January-February 2015 and are shown in Fig. 6 on the main paper. The left column shows the differences between the 2 week moving average biases at January 15 00Z 2015 and the respective mean biases, while the right column shows the same differences but with the 2 week moving averages valid at February 28 00Z 2015. Only differences between bins valid for at the time of the 2 week moving averages as well as in the 2 months average are displayed. The colours blue to purple denote negative differences and the colours yellow to red refer to positive differences.

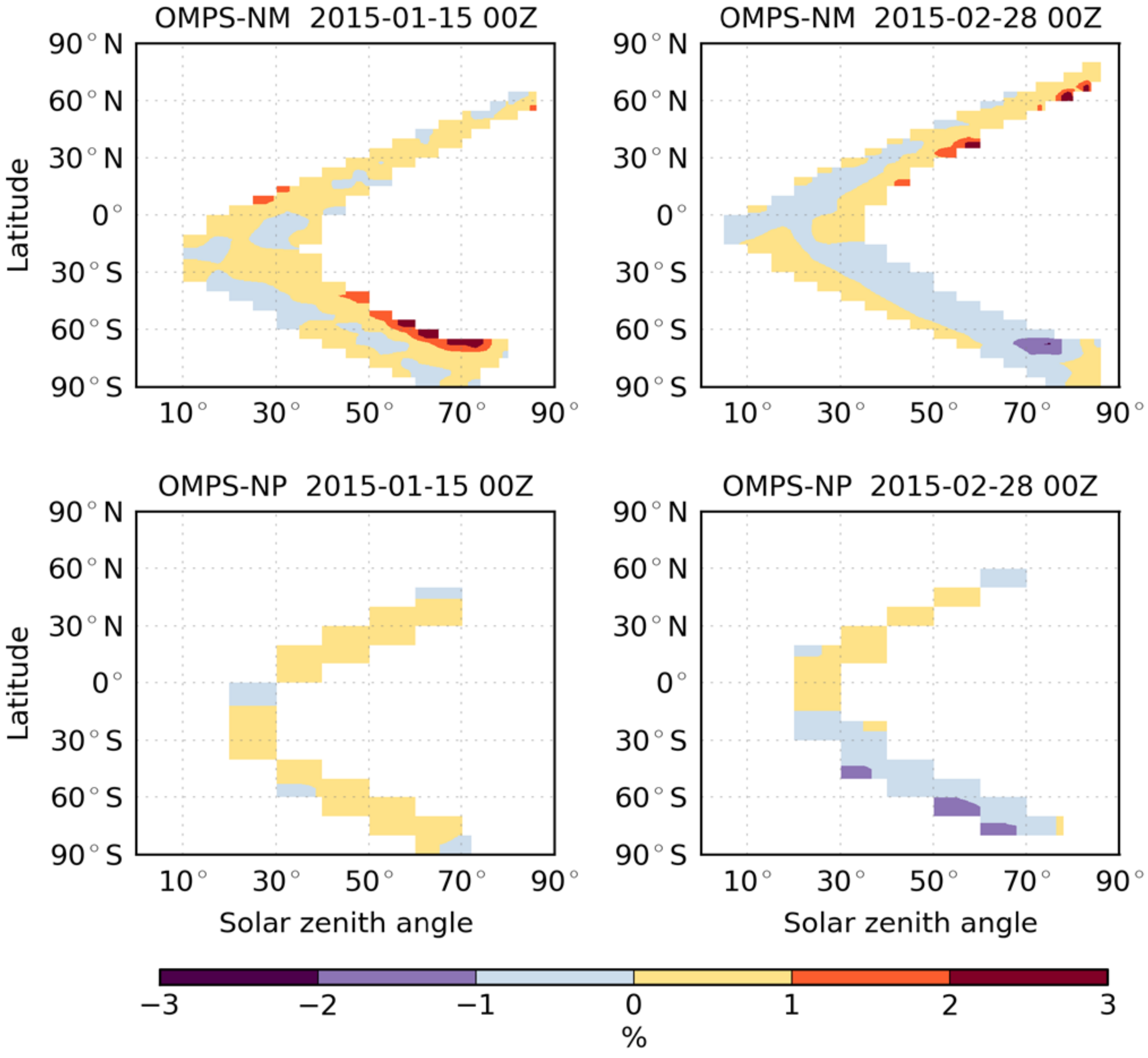

Figure S9. Same as Fig. S8, but where the top and bottom rows displays the differences for OMPS-NM and OMPS-NP, respectively.

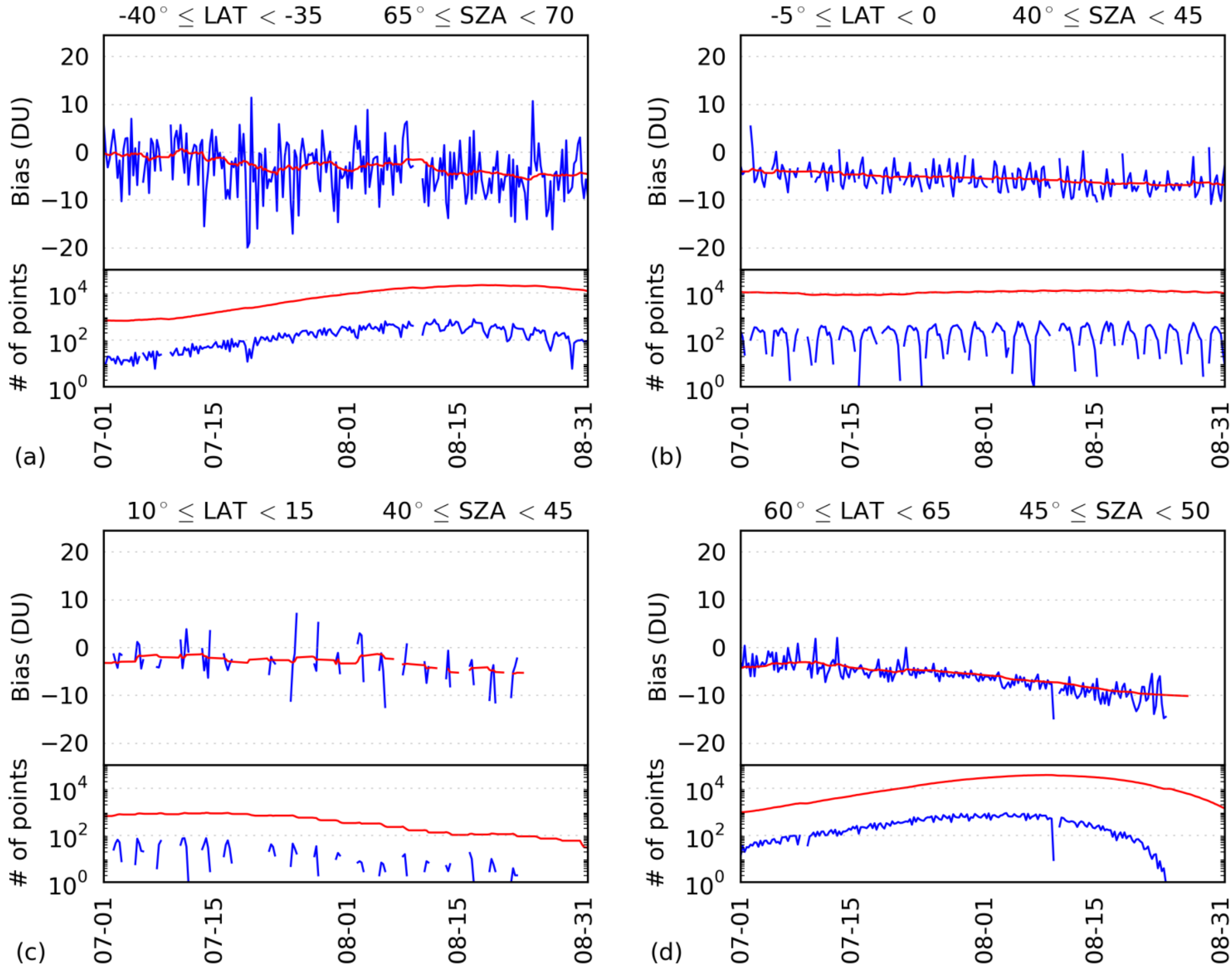

Figure S10. Time series of bias corrections (DU) for GOME-2A, corrected relative to OMI-TOMS, for July and August 2014 for selected latitude/solar zenith angle bins. Panels (a) to (d) show the bias correction for the (latitude, solar zenith angle) bins centred on (37.5°S, 67.5°), (2.5°S, 42.5°), (12.5°N, 42.5°), and (62.5°N, 47.5°), respectively, with a 5° bin width for both the latitude and solar zenith angle. In each panel, the top plot shows the biases and the bottom shows the number of points. The blue lines show individual mean differences from observations gathered in each 6 hour time window from which the bias correction is derived. The red lines show the 2 week moving average bias correction that is applied before assimilation. A gap in the curves denote no data availble at that time.

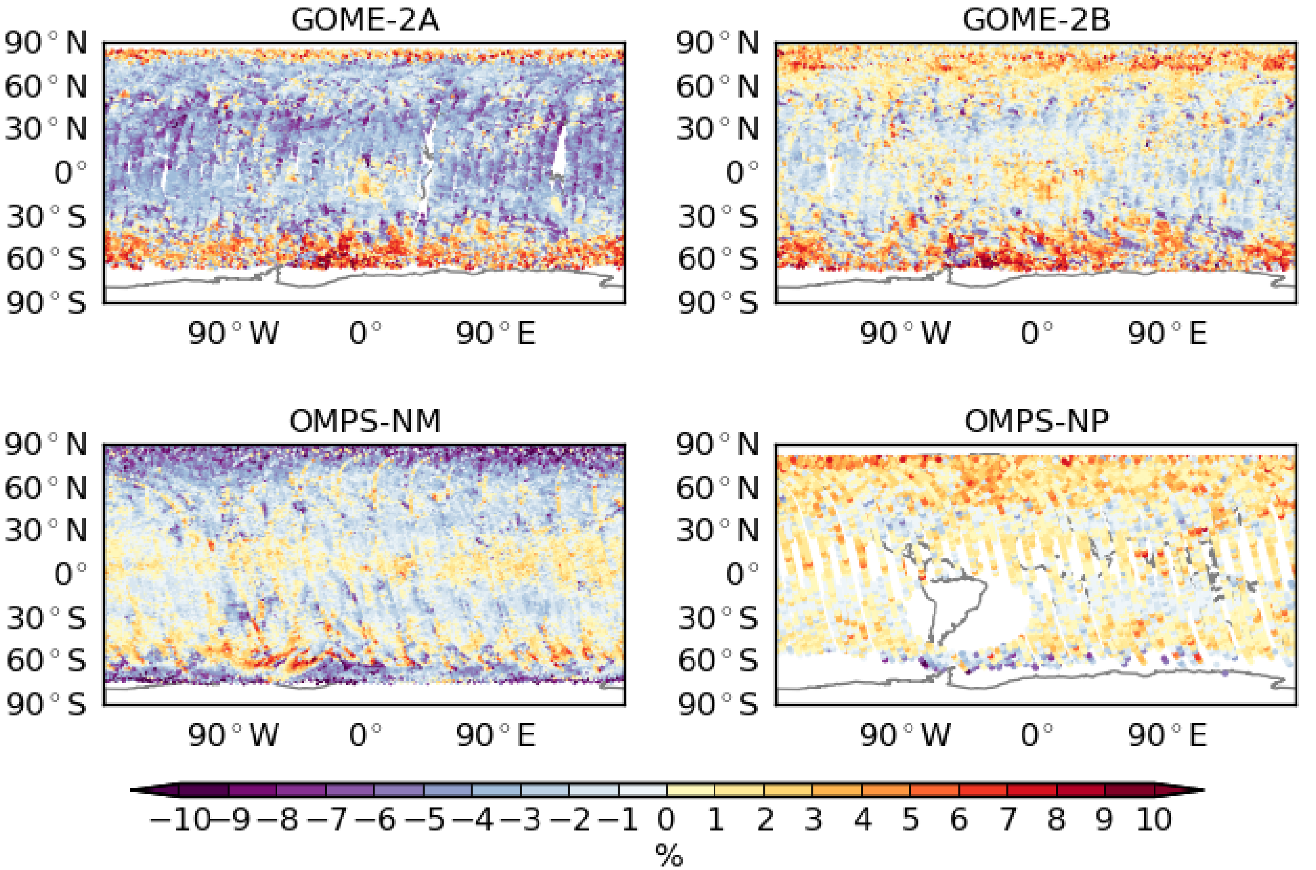

Figure S11. Differences (%) between GOME-2A, GOME-2B, OMPS-NM, and OMPS-NP observations and colocated OMI-TOMS during the time period August 20-29 2014. The colocation criteria are for observations to be within 200 km and 12 h of one another as well as having a difference in latitude of no more than 3° and a maximum solar zenith angle difference of 5° for angles below 70° and 2° above 70°. The colours blue to purple denote negative differences and the colours yellow to red refer to positive differences.

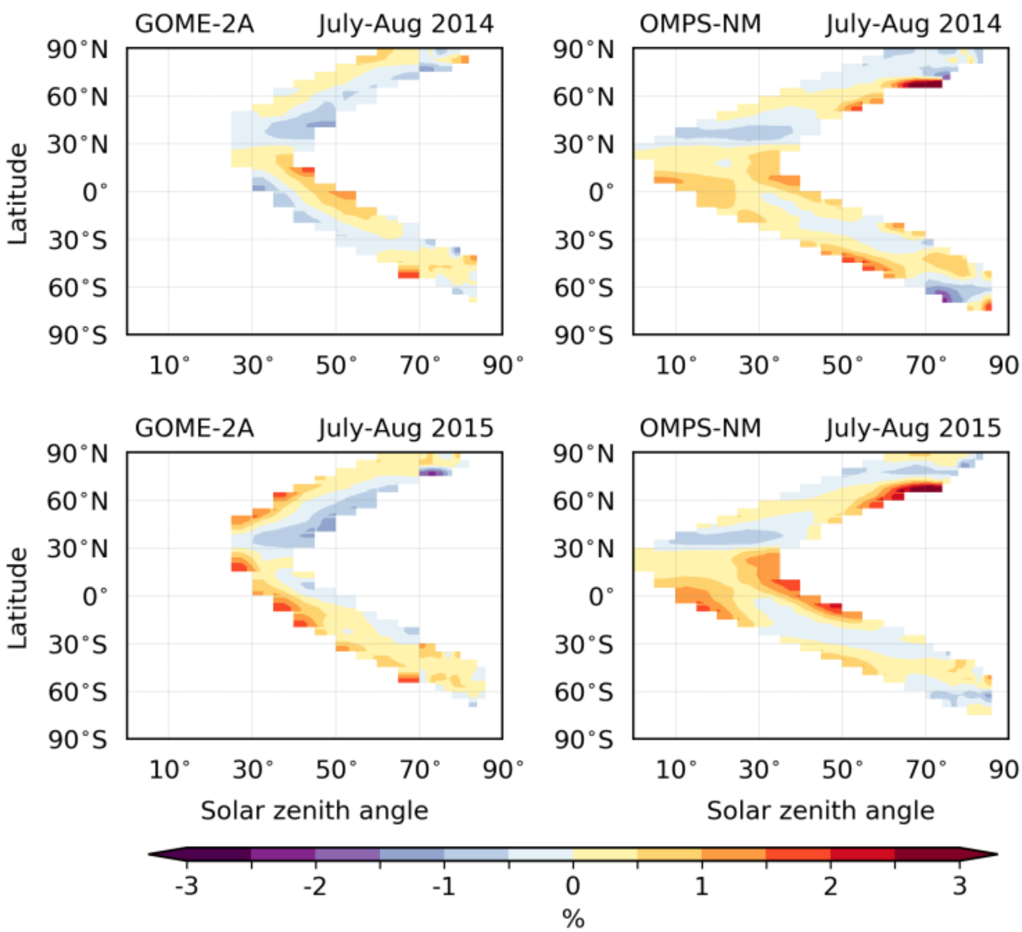

Figure S12. Residual average total column ozone differences (%) between GOME-2A, OMPS-NM and colocated OMI-TOMS data as a function of latitude (degrees) and solar zenith angle (degrees) for July-August 2014 and July-August 2015 following bias correction as a function of ozone effective temperature and solar zenith angle. The colours blue to purple denote negative differences and the colours yellow to red refer to positive differences.

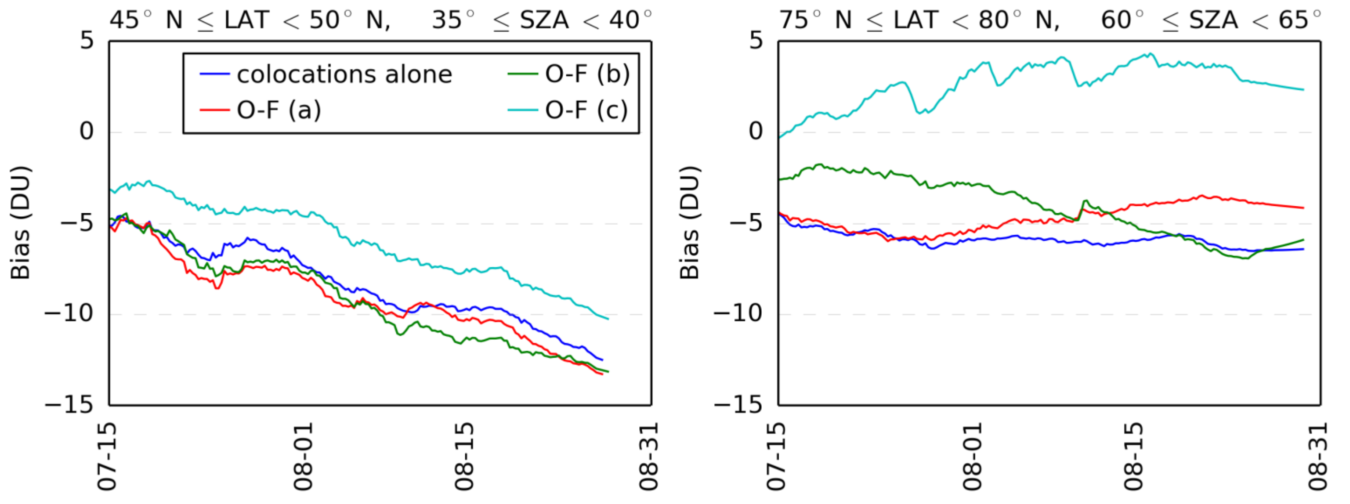

Figure S13. Time series of total column ozone bias corrections (DU) for two latitude/SZA bins covering mid-July to August 2014 for GOME-2A using different bias correction methods. All cases, colocations used the thinned observation sets. The 'O-F' curves additionally use the differences of forecasts described in Section 2.4.4 following the assimilation of uncorrected GOME-2A,B and OMPS-NM.

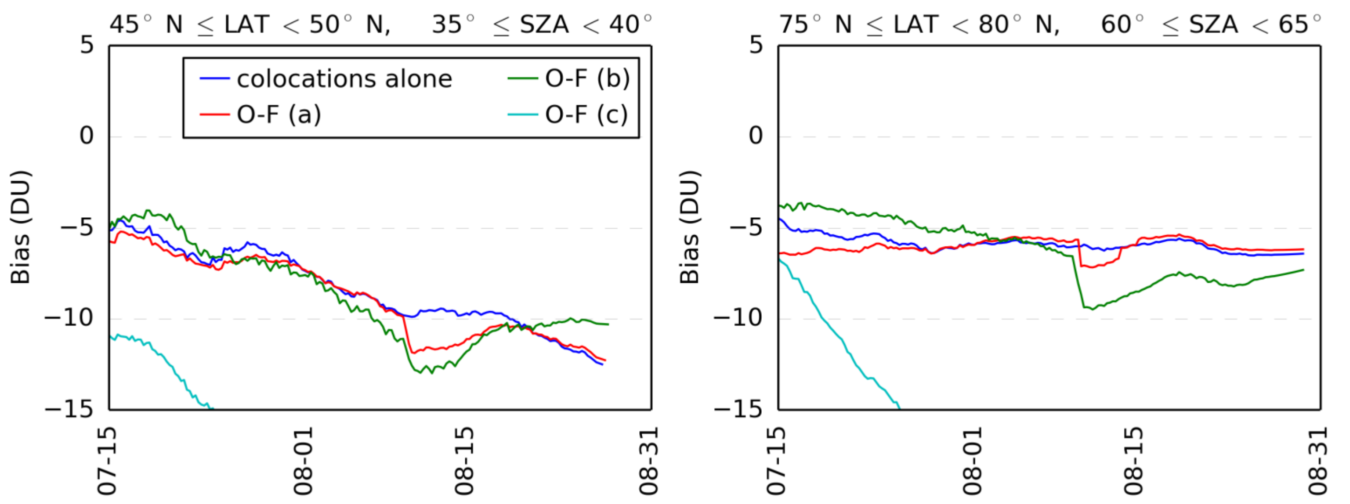

Figure S14. Same as Fig. S13 except the 'O-F' curves use the differences between forecasts made in the absence of assimilation.

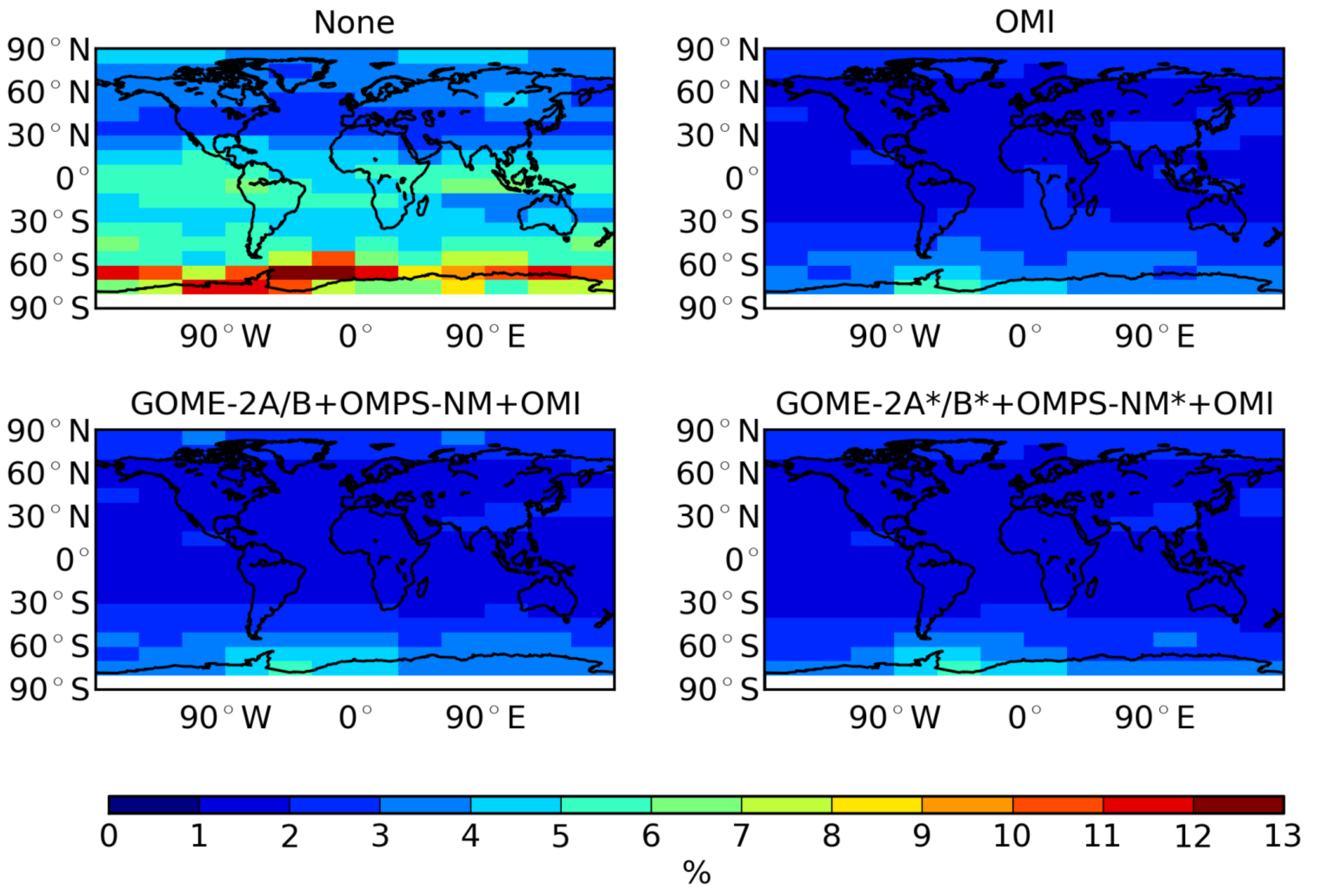

Figure S15. Standard deviations (%) of the differences between OMI-TOMS measurements and six-hour forecasts as a function of spatial location for July-August 2014. The plot titles indicate the instruments assimilated for each run, where an asterisks indicates the assimilation of the bias-corrected set of observations for that instrument. The colours blue to purple denote negative differences and the colours yellow to red refer to positive differences.

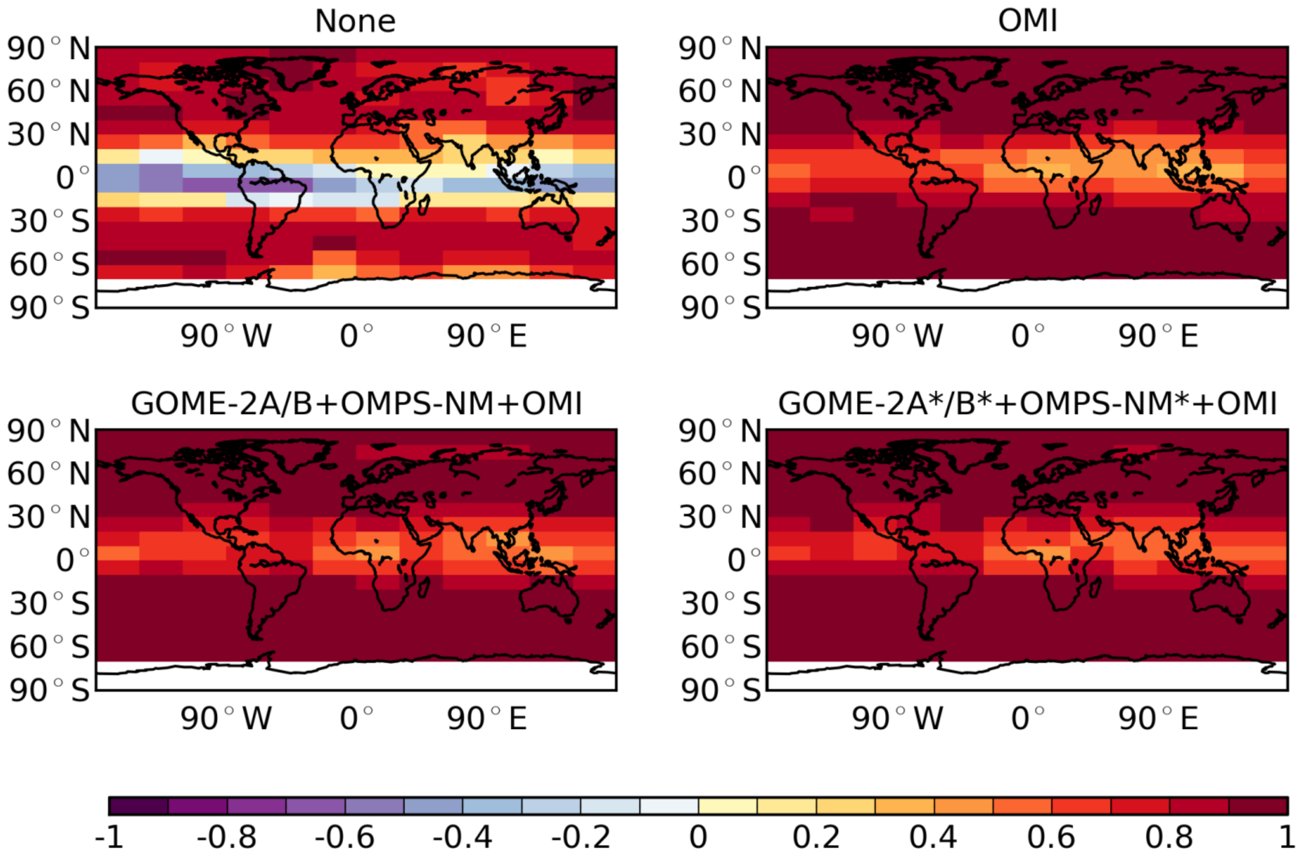

Figure S16. Anomaly correlation coefficients (unitless) between short-term forecasts and OMI-TOMS observations as a function of spatial location for July-August 2014. The plot titles indicate the instruments assimilated for each run, where an asterisks indicates the assimilation of the bias-corrected set of observations for that instrument. The reference field used to calculate the anomaly correlation was the average total column field over the period of July-August 2014 made from the no assimiltion run. The colours blue to purple denote negative differences and the colours yellow to red refer to positive differences.

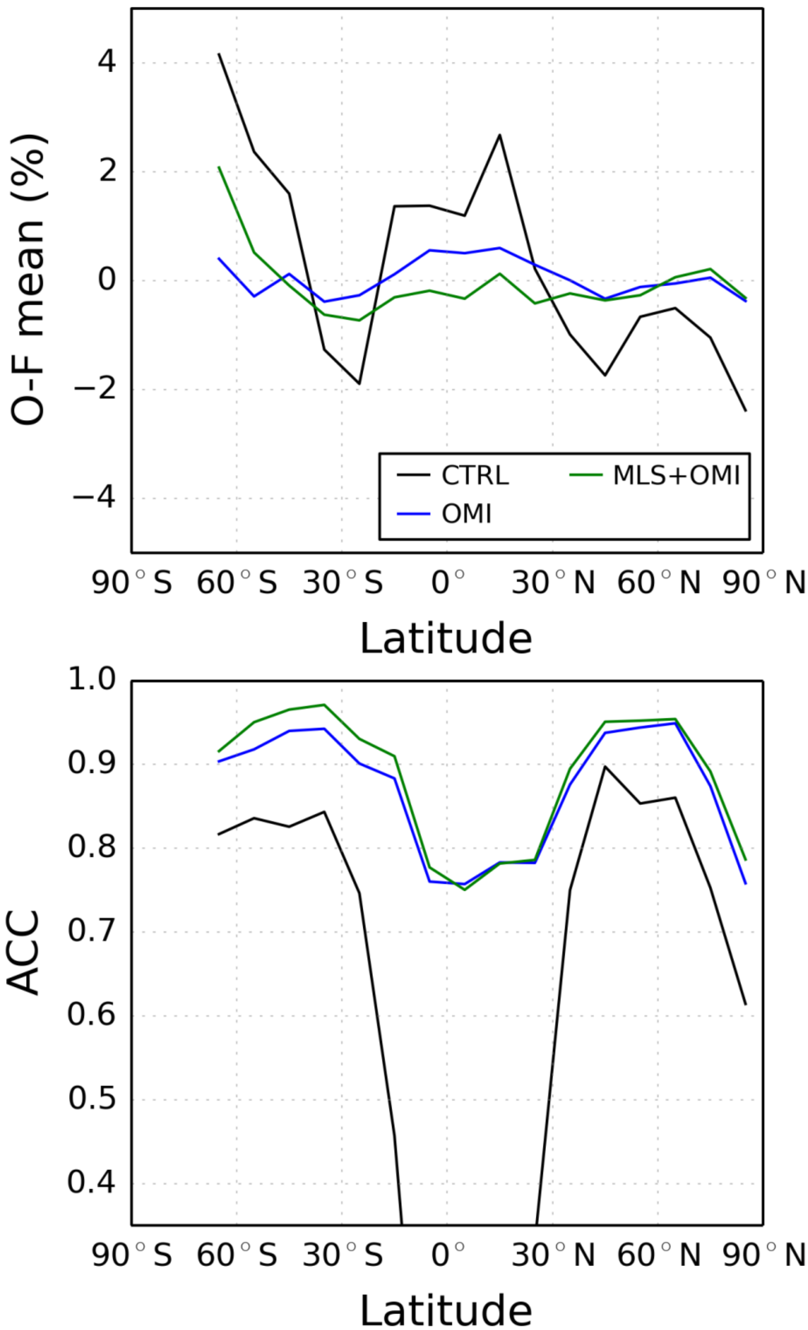

Figure S17. Zonal mean total column ozone differences (%) and anomaly correlaton coefficients (ACC; unitless) between OMI-TOMS observations and short-term forecasts for 1-23 July 2014 showing the effect of assimilating both total column and profile observations. The legend indicates the assimilation run (see Table 2 for description). This shorter period in this figure is imposed by the 'MLS+OMI' assimilation having been conducted only for this duration prior to local computing system changes.

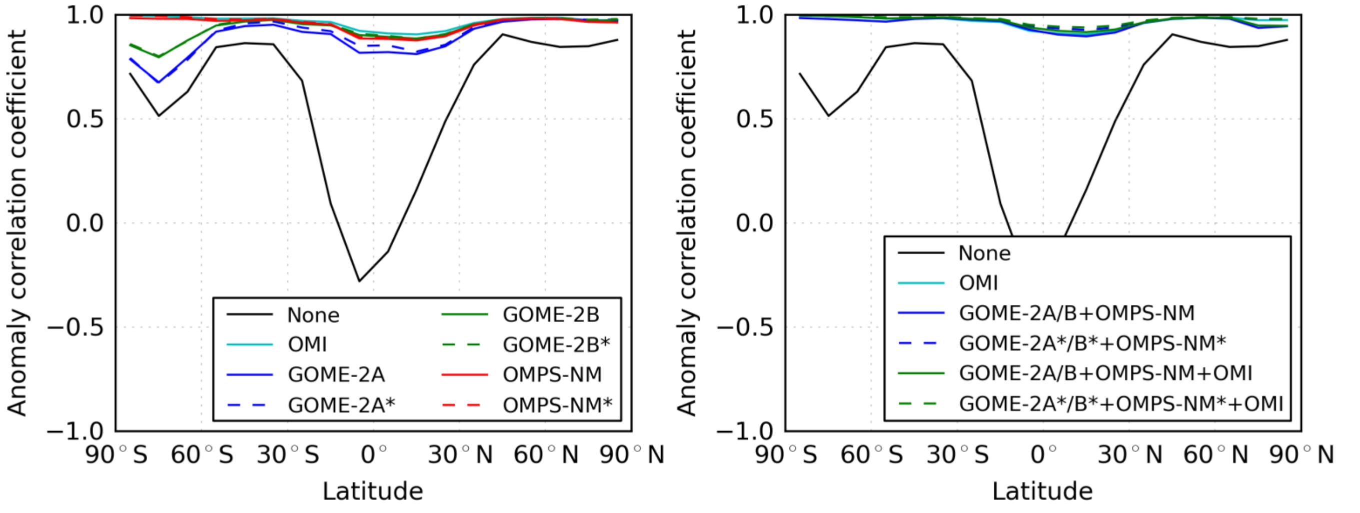

Figure S18. Zonal mean anomaly correlation coefficients (unitless) between short-term forecasts and analyses from the assimilation of the original and bias-corrected GOME-2A/B and OMPS-NM observations as well as OMI-TOMS for July-August 2014. The legend labels indicate the instruments assimilated for each run, where an asterisks indicates the assimilation of the bias-corrected set of observations for that instrument. The reference field used to calculate the anomaly correlation was the average total column field over the period of July-August 2014 made from the no assimiltion run.

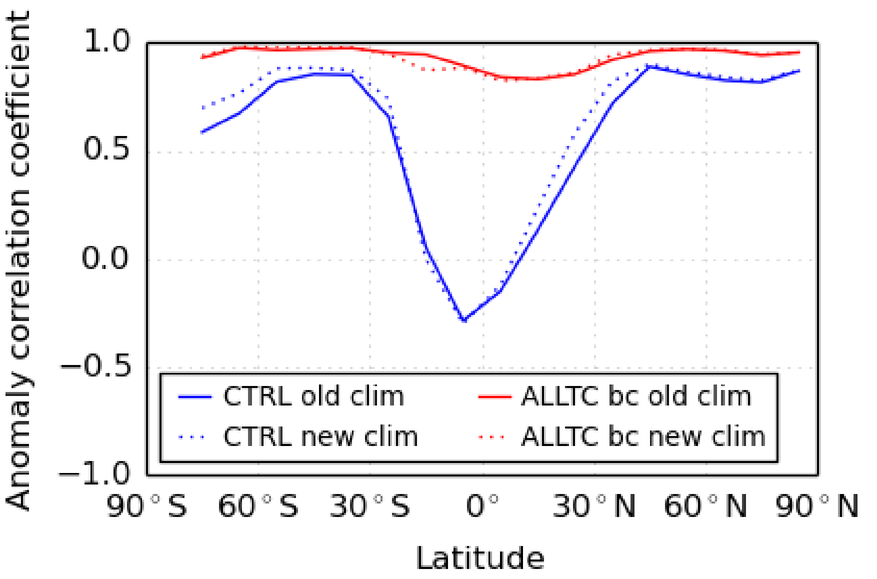

Figure S19. Zonal anomaly correlation coefficients (ACC; unitless) for the comparison between OMI-TOMS measurements and short-term forecasts for July-August 2014 using the July-August 3D average of the CTRL case (referred as the ‘old clim’) as the climatology for all other figures and the August 2D ozone field of Fortuin and Kelder (1998) (referred as the ‘new clim’). The legends indicate the assimilation runs (see Table 2 for description)\

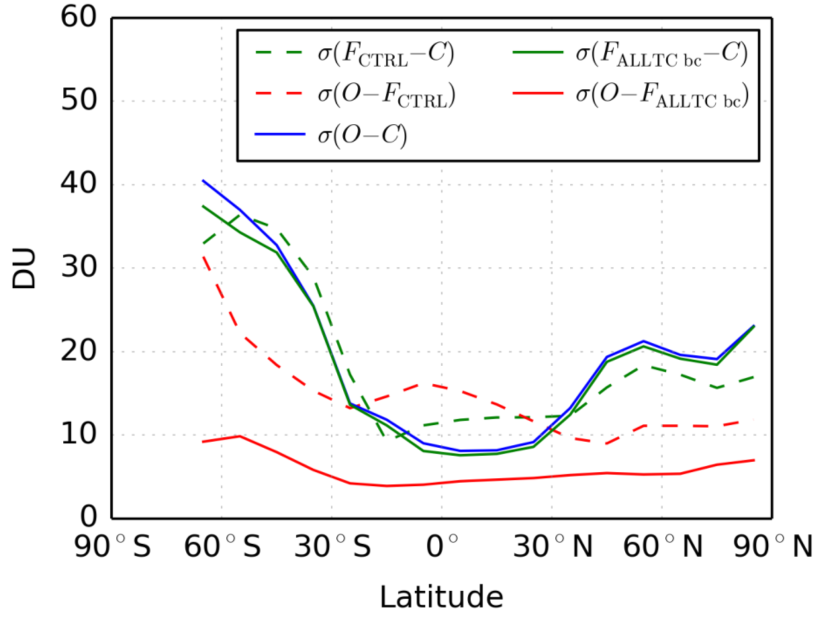

Figure S20. Zonal mean standard derivations (DU) of the differences between short-term forecasts *F*, OMI-TOMS observations *O*, and climatological values *C* over July-August 2014. For the short-term forecasts, the assimilation run from which the forecast was launched is indicated in the subscript, with the labels described in Table 2 of the main paper.